International Journal of Solids and Structures 151 (2018) 2–8

Contents lists available at ScienceDirect

International Journal of Solids and Structures

journal homepage: www.elsevier.com/locate/ijsolstr

On the nonlinear anelastic behavior of AHSS

A. Torkabadi*, E.S. Perdahcıoğlu, V.T. Meinders, A.H. van den Boogaard

Nonlinear Solid Mechanics, Faculty of Engineering Technology, University of Twente, Enschede, The Netherlands

ARTICLE INFO

Article history:
Received 30 November 2016
Revised 3 March 2017
Available online 11 March 2017

Keywords:
Springback
Anelasticity
Dislocations
Nonlinear unloading
AHSS

ABSTRACT

It has been widely observed that the loading/unloading behavior of metals which have previously undergone plastic deformation is nonlinear. Furthermore it shows a hysteresis behavior upon further unloading/reloading cycles. The origin of this nonlinearity is attributed to additional dislocation based micromechanics which contribute to the total reversible strain, referred to as anelastic strain. Compared to a FE model prediction using only elastic contribution to reversible strain the actual springback will be larger. In this work the unloading behavior of DP800 AHSS is analyzed in detail and a mixed physical-phenomenological model is proposed to describe the observed nonlinearity for different levels of pre-strain. This one dimensional uniaxial model is generalized to a 3D constitutive model incorporating elastic, anelastic and plastic strains. The performance of the model is evaluated by comparing the predicted cyclic unloading/reloading stress-strain curves with the experimental ones. It is shown that by incorporating anelastic behavior in the model the prediction of the cyclic behavior of the material is significantly improved.

1. Introduction

There has been an increasing interest by the automotive industry towards employing Advanced High Strength Steels (AHSS) in the past years. However, due to springback, the dimensional accuracy of the components made of AHSS remains an industrial issue (Wagoner et al., 2013). Therefore, an accurate prediction and compensation of the springback are important for utilization of AHSS. Finite element simulations are typically used during the die design stage to estimate the springback in the part. The simulation results are used to adapt the die geometry to compensate for the springback (Burchitz, 2008). The accuracy of such simulations are highly dependent on the constitutive models employed in the simulations that can describe the material behavior during the forming process (Li et al., 2002a).

In the past years most of the research was focused on the development of novel plasticity models to give an accurate stress prediction. On the other hand, little has been done in modeling the material behavior during unloading upon release of the constraining force. The material behavior upon unloading is of importance for the springback prediction considering that the experimental evidence shows that assuming a Hookean behavior to describe the unloading is not realistic. It has been observed experimentally that the material shows a nonlinear unloading/reloading behavior after being plastically deformed (Cleveland and Ghosh, 2002; Eggertsen et al., 2011; Sun and Wagoner, 2011; Eggertsen and Mattiasson, 2010; Govik et al., 2014; Kim et al., 2013; Mendiguren et al., 2013, 2015; Pavlina et al., 2015a, 2015b; Chen et al., 2016b, 2016a). This is caused by an extra reversible strain recovered during unloading along with the pure elastic strain (Cleveland and Ghosh, 2002; Torkabadi et al., 2015; van Liempt and Sietsma, 2016; Arechabaleta et al., 2016). The root cause of this phenomenon has been proposed to be the short-range reversible movement of the dislocations known as anelasticity (Zener, 1948; Ghosh, 1980; Pérez et al., 2005; van Liempt and Sietsma, 2016; Arechabaleta et al., 2016; Chen et al., 2016a). The dislocation structures, which are impeded by the pinning points or piled up before the grain boundaries, can move to a new equilibrium upon the relaxation of the lattice stress and contribute to some extra microscopic strain. From an engineering perspective, considering that the total recovered strain during unloading governs the springback magnitude, it is essential to take into account the anelastic strain in the material models for the FEM springback simulations. In that respect, various researchers have adopted an approach attributed to E-modulus degradation (Morestin and Boivin, 1996; Li et al., 2002b; Yoshida et al., 2002; Yang et al., 2004; Fei and Hodgson, 2006; Yu, 2009; Chongthairungruang et al., 2012). In this approach the E-modulus of the material is made a function of the equivalent plastic strain in the simulations. Hence, the E-modulus represents the chord modulus which is measured from the cyclic experiments. In such experiments, the material is repeatedly plastically deformed to a certain pre-strain and unloaded to zero stress. The chord modulus repre-

* Corresponding author.
E-mail address: a.torkabadi@utwente.nl (A. Torkabadi).

http://dx.doi.org/10.1016/j.ijsolstr.2017.03.009
0020-7683/

sents the slope of the straight line connecting the stress point at the start of unloading to the point at zero stress. The drawback with the E-modulus degradation approach is that it is assumed that all the points in the material are unloaded to zero stress. This is not a realistic assumption in industrial forming processes, where residual stresses are commonly present after unloading, leading to significant errors in springback prediction (Wagoner et al., 2013).

In order to address the above mentioned issue, few attempts have been made in order to model the nonlinear unloading behavior. Eggertsen et al. (2011) and Sun and Wagoner (2011) have taken similar approaches based on the two-yield-surface plasticity theory (Lee et al., 2007) and proposed two-surface constitutive models in which the inner surface defines the transition between the linear and nonlinear elasticity and the outer surface gives the yield criteria. In that way, as long as the stress state is within the inner surface, the stress-strain relation remains linear. This was found in contradiction with the experimental observations (Chen et al., 2016a). On top of that, such models are built based on mathematical convenience rather than capturing the underlying physics of the phenomenon. The model developed by Sun and Wagoner, known as QPE model, has been incorporated with the homogeneous anisotropic hardening (HAH) model by Lee et al. (2013) and a combined isotropic-nonlinear kinematic hardening model by Ghaei et al. (2015) for springback simulations. They found an improvement in the springback prediction capability of the simulations using the QPE model in comparison with the E-modulus degradation approach.

It is therefore the aim of this study to develop a model for the nonlinear unloading behavior of the material for a better springback prediction. This is achieved by first quantifying the anelastic strain by uniaxial tensile tests using sensitive force and displacement measurements. After that a model is developed using the theoretical background of anelasticity in a uniaxial setting which is then generalized into a full 3D constitutive model following conventional continuum plasticity approach. Finally the results are validated by experiments.

2. Experimental procedure

For the experimental part of this study a commercially available DP800 steel grade is used which belongs to the AHSS family. The samples were cut according to ASTM E8 standard from a steel sheet with a thickness of 1 mm in the rolling direction. The tensile tests were conducted using a Zwick/Roell electromechanical universal testing machine and the strain was measured using a custom-made double-sided clip-on extensometer. The double-sided extensometer measures the strain on both sides of the specimen and outputs the average. At low strain levels, misalignment and bending of the sample can have a significant contribution on scatter and uncertainty in the strain measurement which is minimized by averaging the strain measured on both sides of the sample. All the experiments were performed at room temperature.

For the cyclic loading/unloading/reloading experiments (LUR), the controller was programmed to load the specimen to 6000 N and then unload it to zero force. Immediately after the first loading/unloading cycle, the specimen was reloaded to 6500 N of force and unloaded again. This procedure was repeated with increments of 500 N loading until 10 kN of force was reached. The cyclic tests were carried out at a constant crosshead speed of 2, 5 and 10 mm/min which results in strain rates of 0.0002, 0.0005 and 0.001 s^{-1} respectively. The schematic illustration of the experimental procedure is shown in Fig. 1. For every strain rate the experiment was performed on three specimens.

The hardening parameters of the material were determined from the monotonic tensile experiment. The specimen was strained

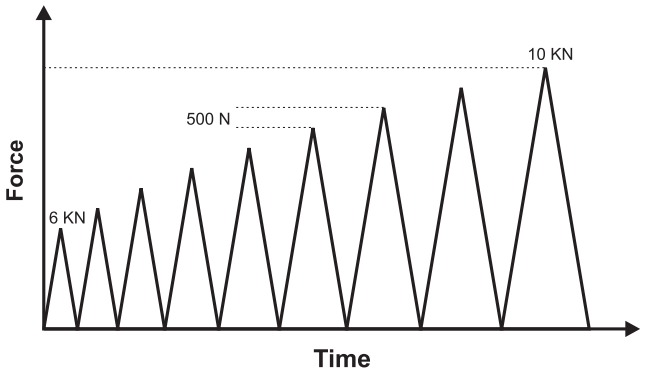

Fig. 1. Schematic illustration of the LUR experimental procedure.

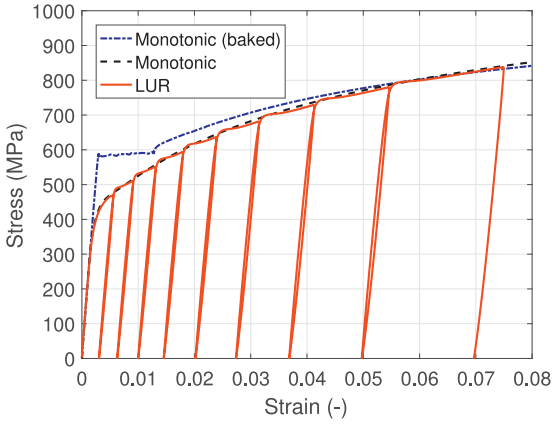

Fig. 2. Experimental stress-strain curves.

up to 15% engineering strain at a constant crosshead speed of 5 mm/min resulting in a strain rate of 0.0005 s^{-1}.

In order to determine the pure E-modulus, the specimen was first baked at 220 °C for 20 min which theoretically should eliminate the anelastic behavior due to pinning of dislocations. Next, the specimen was strained up to 15% and the E-modulus of the specimen was determined according to ASTM E111 standard. The same pre-strained specimen was baked at the same condition once again and the E-modulus was reevaluated according to the same procedure. After every baking treatment, the specimen was first naturally cooled down to room temperature before the tensile test. The experiment was repeated with three specimens.

3. Experimental results

The stress-strain curves obtained from the monotonic (for the baked and as-received specimens) and cyclic (LUR) tensile experiments are shown in Fig. 2.

Comparing the tensile experiment results of the as-received and the baked specimens it is clear that the upper yield point and the yield point elongation phenomena are restored in the baked specimen. Such phenomena are associated with the lack of mobile dislocations in the material. At high temperatures interstitial solute atoms such as carbon can diffuse to the dislocation lines and pin them (Cottrell and Bilby, 1949). In this way when the material is loaded, the dislocations movement is confined and therefore the anelastic strain vanishes. Hence, the slope of the stress strain curve represents the pure elastic modulus. In this context this value is referred to as the E-modulus. To check whether the E-modulus of the baked specimen is affected by pre-straining, the same specimen (after 15% pre-strain) was baked at the same condition (at 220 °C for 20 min) and the E-modulus was re-evaluated. The stress-strain plots of the baked specimen before straining and the baked spec-

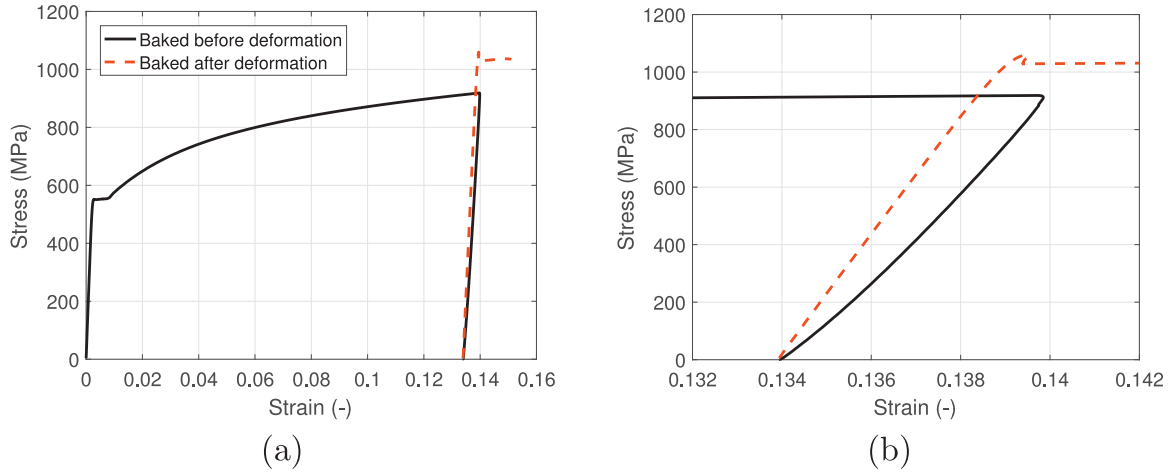

Fig. 3. (a) The stress-strain curve of the specimen after baking and baking after deformation; (b) magnified view of the stress-strain curves at the point of unloading and reloading after baking.

imen after 15% pre-straining are plotted in Fig. 3. The magnified view of the stress-strain curve in Fig. 3b clearly shows that the nonlinear behavior during reloading is vanished after baking the deformed specimen.

The averaged E-modulus (from three experiments) of the as-received baked specimens where found to be 204 ± 3 GPa and 202 ± 6 GPa for the pre-strained baked specimens. To check if there is a significant difference between the two means, the *t*-test under the null assumption was performed on both populations. T-test is a statistical method to determine if there is a significant difference between two sets of data (Montgomery et al., 2011). The outcome of the *t*-test suggests that there is no evidence on the reduction of the E-modulus with plastic deformation. This evidence invalidates the claim made by researchers who relate the nonlinear unloading/reloading cycles and the reduction of chord modulus to damage (Yeh and Cheng, 2003; Halilovič et al., 2007; Vrh et al., 2008; Halilovič et al., 2008; Vrh et al., 2011). Moreover, this further confirms the role of dislocations in the nonlinear behavior.

Classically the LUR experiments are used to characterize the nonlinear unloading behavior of the material with plastic deformation. The results obtained from such experiments are only valid if the material behavior is not altered by the unloading cycles. Comparing the stress-strain curves obtained from the monotonic tensile experiment with LUR experiments, it can be concluded that the hardening behavior of the material is not affected by the unloading cycles.

A magnified view of a typical LUR cycle is shown in Fig. 4 which corresponds to the 7th cycle of the LUR experiment. The graphical representation of the chord modulus as well as the decomposition of the total reversible strain into the elastic and anelastic parts are shown in Fig. 4.

The reduction of the chord modulus as a function of the pre-strain for different strain rates is plotted in Fig. 5. Various authors have reported the reduction of the chord modulus with plastic pre-strain and have developed analytical functions to describe this reduction (Yoshida et al., 2002; Li et al., 2002b; Yang et al., 2004; Fei and Hodgson, 2006; Zang et al., 2007; Yu, 2009; Liu et al., 2013).

For the first unloading cycle at 0.5% pre-strain, the chord modulus is around 183 GPa which is significantly lower than the elastic modulus of the baked specimens (*i.e.* 204 GPa). The chord modulus continues to decrease to approximately 155 GPa after 8% plastic strain. This reveals the significance of such analysis for accurate springback prediction in forming processes.

To describe the nonlinear anelastic behavior firstly a relation for the total recoverable anelastic strain should be established. Considering that the total reversible strain (ε^{rev}) is partially elastic (ε^{e}) and partially anelastic (ε^{an}), the contribution of the anelastic strain can be determined by subtracting the elastic strain from the entire recovered strain

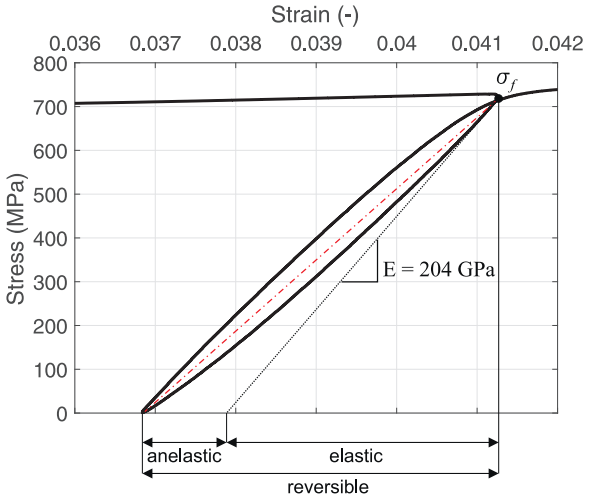

Fig. 4. Magnified view of the 7th unloading/reloading cycle. The E-modulus is determined from the bake-hardened samples and the chord modulus is obtained by connecting the starting and end point of unloading with a straight line.

$$\varepsilon_t^{an} = \varepsilon_t^{rev} - \varepsilon_t^{e} = \varepsilon_t^{rev} - \frac{\sigma_f}{E} \tag{1}$$

where E is the elastic modulus of the baked material (*i.e.* 204 GPa) and subscript t refers to the total strain recovered when the material is unloaded to zero stress. The total recovered anelastic strain is plotted against the flow stress in Fig. 6 for different strain rates. Based on the results, no strong conclusion can be drawn on the strain rate dependency of the anelastic strain in the range it was evaluated. While the chord modulus decreases, the anelastic strain increases as the material hardens.

4. The model

A number of studies on the nonlinear unloading behavior used the dislocation density to quantitatively describe the phenomenon (Mott, 1952; Friedel, 1953; Kim et al., 2013; Torkabadi et al., 2015; van Liempt and Sietsma, 2016). Hull and Bacon (2011) state that the magnitude of the recoverable anelastic strain is proportional to

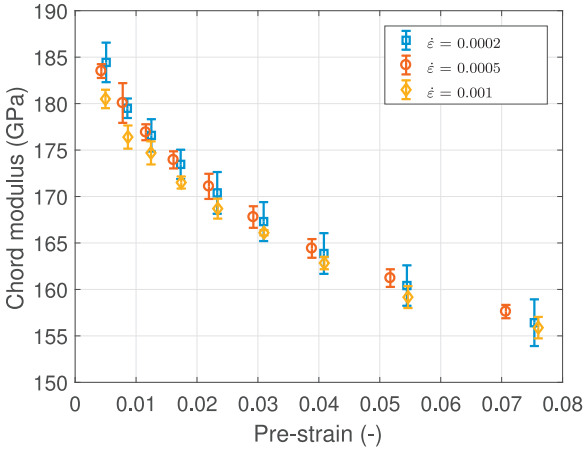

Fig. 5. Variation of the chord modulus with plastic pre-strain.

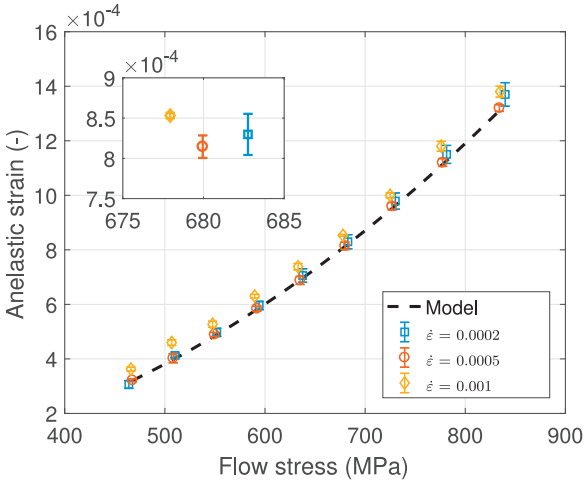

Fig. 6. Variation of the total recovered anelastic strain with unloading stress.

the dislocation density according to

$$\varepsilon^{an} = \rho b \bar{x} \tag{2}$$

where ρ is the dislocation density, b is the Burgers vector and $\bar{x}$ is the average distance moved by dislocations. As the material plastically deforms, the dislocation density increases which leads to an increase in the flow stress. The Taylor equation is one of the most established expressions relating the flow stress of a material to its dislocation density (Taylor, 1934) according to

$$\sigma_f = \sigma_0 + \bar{M}\alpha G b\sqrt{\rho} \tag{3}$$

where $\bar{M}$ is the Taylor factor, α is the dislocation strengthening parameter and a material related constant, G is the shear modulus of the material, ρ is the dislocation density and σ_0 is the lattice friction stress of the material in the absence of dislocation interactions. In order to replace σ_0 with the flow stress of the as-received material σ_{y0}, Eq. (3) can be rewritten as (Viguier, 2003)

$$\sigma_f = \sigma_{y0} + \bar{M}\alpha G b(\sqrt{\rho} - \sqrt{\rho_0}) \tag{4}$$

where ρ_0 is the dislocation density of the material when it becomes plastically deformed at σ_{y0}. Rewriting Eq. (4) yields an expression for dislocation density evolution as a function of hardening behavior of the material according to

$$\rho = \left(\frac{\sigma_f - \sigma_{y0}}{\bar{M}\alpha G b} + \sqrt{\rho_0}\right)^2 \tag{5}$$

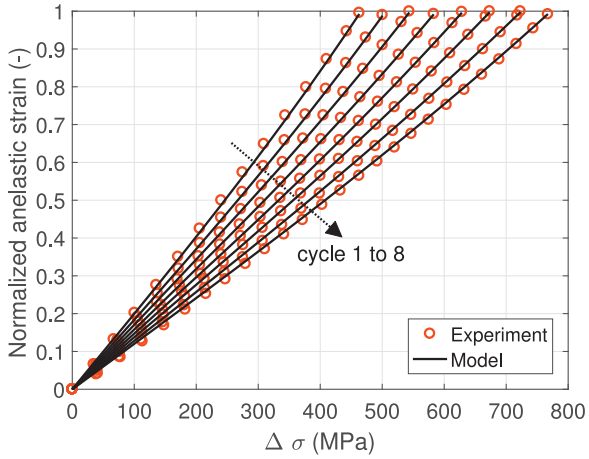

Fig. 7. Normalized anelastic strain ($\varepsilon^{an}/\varepsilon_t^{an}$) as a function of unloading stress.

Using Eq. (5) in combination with Eq. (2), the evolution of the anelastic strain is given as a function of the work hardening behavior of the material as

$$\varepsilon_t^{an} = \left(K(\sigma_f - \sigma_{y0}) + \sqrt{\varepsilon_0^{an}}\right)^2 \tag{6}$$

where K is a material parameter and ε_0^{an} is the magnitude of the anelastic strain proportional to the initial dislocation density ρ_0. The parameter K, with the dimension of reciprocal stress (Pa^{-1}), determines how the anelastic strain evolves as a function of the flow stress. For the higher values of K the curvature of the curve giving the anelastic strain to the flow stress (i.e. Fig. 6) increases. The value of K can be determined by fitting Eq. (6) to the experimental data in Fig. 6 taking $\sigma_{y0} = 460$ MPa. It should be noted that the fitting was performed only on the data set obtained from experiments of 0.0005 s^{-1} strain rate. The details on deriving Eq. (6) is given in Torkabadi et al. (2015).

The total recoverable anelastic strain upon unloading to zero stress is given by Eq. (6). Yet, another equation is needed to describe the nonlinearity upon unloading. A phenomenological approach is taken to identify the function describing nonlinearity. From the experimental results it has been found that unloading behavior can be well described according to

$$\varepsilon^{an} = \left(K(\sigma_f - \sigma_{y0}) + \sqrt{\varepsilon_0^{an}}\right)^2 \frac{\sinh(\kappa s)}{\sinh(\kappa)} \tag{7}$$

here κ is a fitting parameter and s is the dimensionless normalized stress defined as

$$s = \frac{|\Delta\sigma|}{\sigma_f} \tag{8}$$

where $\Delta\sigma$ is the stress decrement upon unloading from the flow stress.

The value of κ was obtained from fitting Eq. (7) to the experimental data shown in Fig. 7 using the least squares method using all the unloading cycles. As a simplification to the model, the nonlinear reloading curve is assumed to be symmetric with the unloading curve along the chord modulus line. Hence, the reloading curve can be described using the same function taking $\Delta\sigma$ in Eq. (8) as the increment of stress from zero stress. The anelastic model parameters are summarized in Table 1.

In order to describe the anelastic model in terms of the equivalent plastic strain ε_{eq}^p, σ_f in Eq. (7) can be substituted with a hardening law. For simplicity, the Swift hardening law is used which is given as

$$\sigma_f = C\left(\varepsilon_0 + \varepsilon_{eq}^p\right)^n \tag{9}$$

Table 1
Anelastic model parameters for DP800.

$\varepsilon^{an} = (K(\sigma_f - \sigma_{y0}) + \sqrt{\varepsilon_0^{an}})^2 \frac{\sinh(\kappa s)}{\sinh(\kappa)}$			
K (MPa^{-1})	σ_{y0} (MPa)	ε_0^{an}	κ
5.1×10^{-5}	430	3×10^{-4}	0.68

Table 2
Swift hardening parameters for DP800.

$\sigma_f = C(\varepsilon_0 + \varepsilon_{eq}^p)^n$		
C (MPa)	ε_0	n
1710	0.0072	0.28

The monotonic tensile experiment was used to determine the parameters for the Swift hardening law. These parameters are given in Table 2.

5. Constitutive modeling

In order to implement the model in a FEM code, the constitutive rate equations are required. Additive decomposition of the total strain rate into elastic $\dot{\boldsymbol{\varepsilon}}^e$, anelastic $\dot{\boldsymbol{\varepsilon}}^{an}$ and plastic $\dot{\boldsymbol{\varepsilon}}^p$ strain rates yields

$$\dot{\boldsymbol{\varepsilon}} = \begin{cases} \dot{\boldsymbol{\varepsilon}}^e + \dot{\boldsymbol{\varepsilon}}^{an}, & \text{if } \phi < 0 \\ \dot{\boldsymbol{\varepsilon}}^e + \dot{\boldsymbol{\varepsilon}}^{an} + \dot{\boldsymbol{\varepsilon}}^p, & \text{if } \phi = 0 \end{cases} \tag{10}$$

where ϕ is the yield function. The rate of the elastic strain is given according to

$$\dot{\boldsymbol{\varepsilon}}^e = \mathbb{E}^{-1} : \dot{\boldsymbol{\sigma}} \tag{11}$$

where $\mathbb{E}$ is the isotropic elasticity tensor. For Drucker postulated associated flow, the rate of plastic strain is given as

$$\dot{\boldsymbol{\varepsilon}}^p = \dot{\lambda} \frac{\partial \phi}{\partial \boldsymbol{\sigma}} \tag{12}$$

Assuming the same flow potential for the anelastic strain, the rate of the anelastic strain can be written as

$$\dot{\boldsymbol{\varepsilon}}^{an} = \dot{\xi} \frac{\partial \phi}{\partial \boldsymbol{\sigma}} \tag{13}$$

where the scalar multiplier $\dot{\xi}$ can be written as

$$\dot{\xi} = \frac{3}{2} \dot{\varepsilon}^{an} \tag{14}$$

Here $\dot{\varepsilon}^{an}$ is the time derivative obtained from Eq. (7).

The assumption of the associated flow rule is justified supposing that the anelastic strain is resulted from the motion of dislocations distributed in a polycrystalline material under the action of stress. The dislocations contributing to the anelastic strain were generated and oriented on the slip planes which were activated during the plastic deformation. Therefore, it is assumed that the net anelastic strain rate tensor is collinear with the normal of the yield function.

In order to model the hysteretic behavior observed in unloading/reloading cycles, a load reversal criterion is introduced. Accordingly, the value of s in Eq. (7) is evaluated as

$$s = \int \dot{s}\, dt \tag{15}$$

where the integral is evaluated from the time when the load reversal starts which is determined using the criterion

$$\frac{\dot{\boldsymbol{\sigma}}_n}{|\dot{\boldsymbol{\sigma}}_n|} : \frac{\dot{\boldsymbol{\sigma}}_{n+1}}{|\dot{\boldsymbol{\sigma}}_{n+1}|} < 0 \tag{16}$$

Eq. (16) implies that the load reversal condition is satisfied when the relative angle between the two successive stress increments exceeds $\frac{\pi}{2}$ (Nguyen et al., 2013).

Clearly, this formulation is independent of the flow function and the hardening law; however, for demonstration of the model the von Mises flow function and the Swift hardening law are incorporated in the following.

For the implementation of the model an implicit, backward Euler type numerical scheme is used for return mapping that is proposed by Wilkins (1963). More details on the formulations can also be found in Simo and Hughes (2006).

6. Model validation

In order to evaluate the performance of the proposed model in predicting the nonlinear unloading/reloading cycles, the stress-strain curves obtained from the model and the LUR experiment are compared. The stress-strain curves obtained from the model and the experiment are plotted in Fig. 8. A magnified view of the 5th, 6th and 7th cycles are given in Fig. 8b–d, respectively. For comparison, the unloading path predicted by the chord modulus and E-modulus are plotted alongside the anelastic model in Fig. 8d.

As can be seen in Fig. 8, the predicted unloading curve using the anelastic model is very well in agreement with the experimental data; whereas, the unloading path obtained by purely elastic unloading and unloading using the chord modulus respectively tend to underpredict and overpredict the strain during unloading.

The difference between the strain from the model prediction and from the experimental data is used as a measure of error. The root mean square (RMSE) of the strain deviation is given as

$$\text{RMSE} = \sqrt{\frac{\sum_{i=1}^{n} e_i^2}{n}} \tag{17}$$

where e_i is the difference between the strain predicted by the model and the experimental data at the ith data point during unloading.

The strain deviation between the experimental data and the prediction of each model for the 7th unloading cycle is plotted in Fig. 9a. Clearly the highest deviation from the experimental data is seen in case of using the pure elastic model to predict the unloading behavior. The chord modulus approximation only yields an exact prediction at the start of unloading and at zero stress while for the points that were unloaded halfway the chord modulus is not accurate. This is a source of error in springback prediction of an industrial forming process where some residual stresses are present in the part after the springback. It can be clearly seen that this error has been significantly reduced using the nonlinear anelastic model.

The RMSE obtained from the unloading curves at different plastic pre-strains are plotted in Fig. 9b. As shown in Fig. 9a, the error in strain prediction during unloading using the linear pure elastic unloading approach increases with increase of the plastic strain. This error is significantly lower in case of taking the chord modulus approach. Lastly, the unloading curve predicted by the anelastic model shows a very small deviation from the experimental data comparing to the other two approaches. The RMSE stays below 0.00005 for plastic strains up to 5.5%. A comparison between the sum of the RMSEs of all the cycles for each approach suggests that using the proposed model, an improvement by a factor of 8 and 14 is obtained in comparing with the chord modulus and E-modulus approaches respectively.

7. Conclusions

In this work a series of monotonic and LUR uniaxial tensile experiments were conducted on DP800 from the family of AHSS.

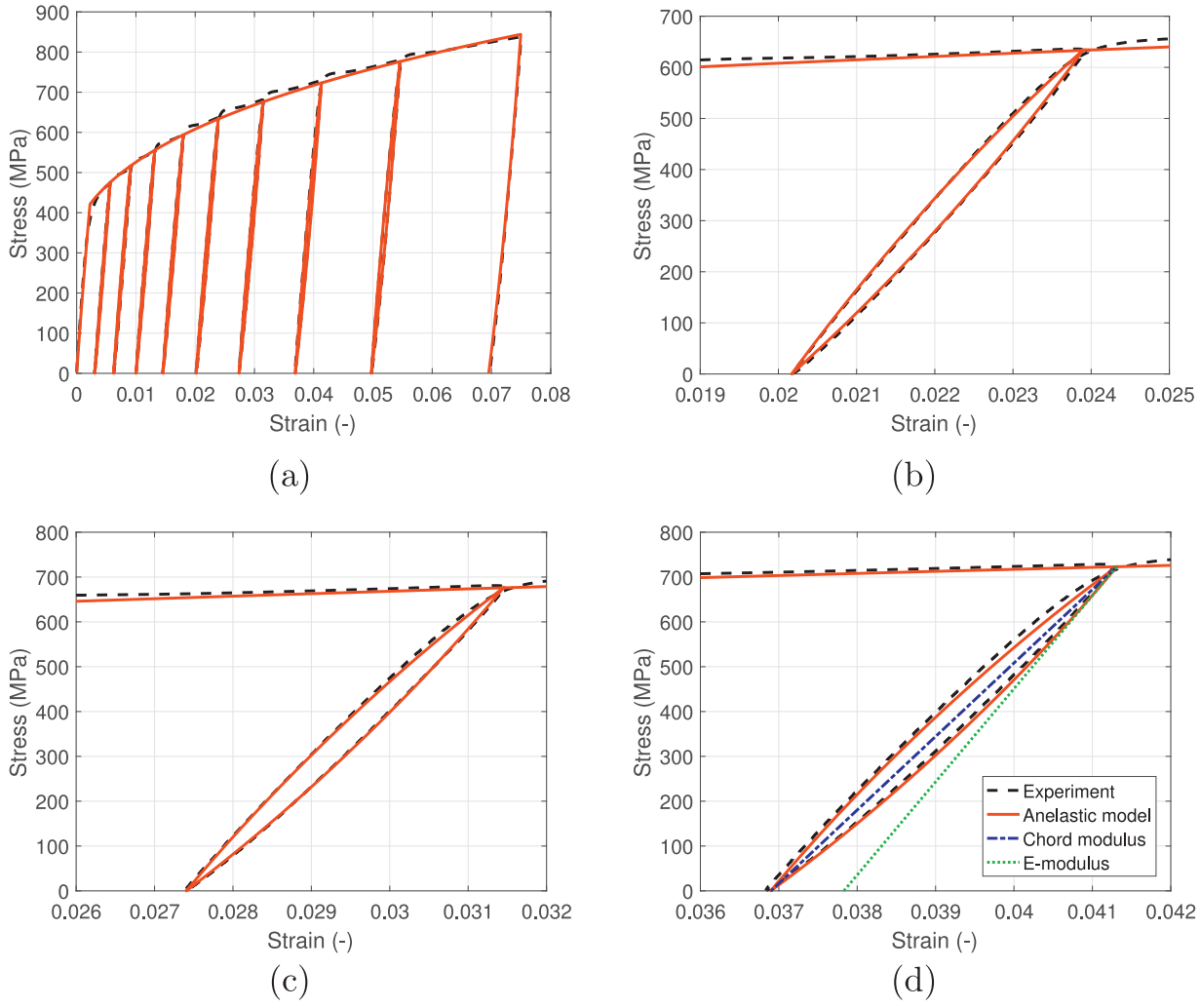

Fig. 8. Stress-strain response of DP800 (a) Complete LUR; magnified view of the (b) 5th cycle, (c) 6th cycle and (d) 7th cycle.

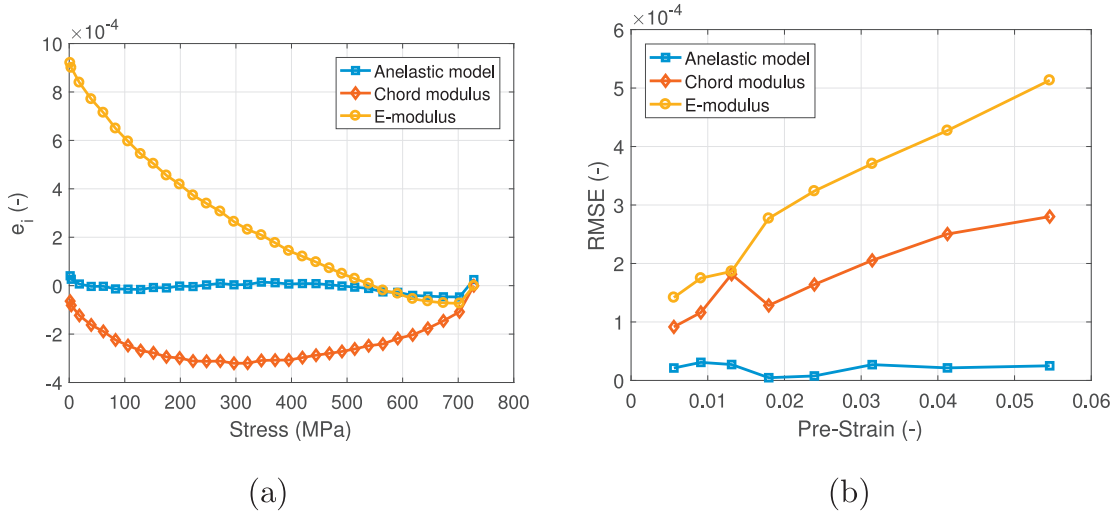

Fig. 9. (a) The strain deviation between the experiment and the prediction of anelastic model, chord modulus and E-modulus; (b) RMSE of strain prediction during unloading for the anelastic model, chord modulus and E-modulus.

Tensile experiments on baked specimens were conducted to measure the E-modulus and to investigate the nature of the nonlinear behavior. The tensile experiments conducted on the as-received and pre-strained baked specimens revealed that the dislocation based micro-mechanics are responsible for the observed nonlinearity. Furthermore, a 1D mixed physical-phenomenological model was developed to describe the nonlinear behavior. This model was generalized to a 3D constitutive model considering the anelastic strain rate tensor co-directional with the plastic strain rate. The model was calibrated to the experimental data obtained from LUR experiments. Comparing the model prediction with the experimental data showed a significant improvement over strain prediction incorporating the anelastic behavior. Hence, using the proposed model in FE simulations of forming processes will result in better prediction of the residual stresses and thus springback behavior of complex parts.

Acknowledgments

This research was carried out under project number S22.1.13494a in the framework of the Partnership Program of the Materials innovation institute M2i (www.m2i.nl) and the Technology Foundation STW (www.stw.nl), which is part of the Netherlands Organization for Scientific Research (www.nwo.nl).

The authors acknowledge the support of Tata Steel in this project with material and in particular the discussions with Peter van Liempt, Pascal Kömmelt and Eisso Atzema.

References

Arechabaleta, Z., van Liempt, P., Sietsma, J., 2016. Quantification of dislocation structures from anelastic deformation behaviour. Acta Mater. 115, 314–323.
Burchitz, I.A., 2008. Improvement of springback prediction in sheet metal forming. Ph.D. thesis. Enschede, The Netherlands.
Chen, Z., Bong, H.J., Li, D., Wagoner, R.H., 2016a. The elasticplastic transition of metals. Int. J. Plast. 83, 178–201.
Chen, Z., Gandhi, U., Lee, J., Wagoner, R.H., 2016b. Variation and consistency of youngs modulus in steel. J. Mater. Process. Technol. 227, 227–243.
Chongthairungruang, B., Uthaisangsuk, V., Suranuntchai, S., Jirathearanat, S., 2012. Experimental and numerical investigation of springback effect for advanced high strength dual phase steel. Mater. Des. 39, 318–328.
Cleveland, R.M., Ghosh, A.K., 2002. Inelastic effects on springback in metals. Int. J. Plast. 18 (56), 769–785.
Cottrell, A.H., Bilby, B.A., 1949. Dislocation theory of yielding and strain ageing of iron. Proc. Phys. Soc. Sect. A 62 (1), 49–62.
Eggertsen, P.A., Mattiasson, K., 2010. On constitutive modeling for springback analysis. Int. J. Mech. Sci. 52 (6), 804–818.
Eggertsen, P.A., Mattiasson, K., Hertzman, J., 2011. A phenomenological model for the hysteresis behavior of metal sheets subjected to unloading/reloading cycles. J. Manuf. Sci. Eng. 133 (6), 061021.
Fei, D., Hodgson, P., 2006. Experimental and numerical studies of springback in air v-bending process for cold rolled TRIP steels. Nucl. Eng. Des. 236 (18), 1847–1851.
Friedel, J., 1953. Xlvi. anomaly in the rigidity modulus of copper alloys for small concentrations. London Edinburgh Dublin Philosoph. Mag. J. Sci. 44 (351), 444–448.
Ghaei, A., Green, D.E., Aryanpour, A., 2015. Springback simulation of advanced high strength steels considering nonlinear elastic unloadingreloading behavior. Mater. Des. 88, 461–470.
Ghosh, A.K., 1980. A physically-based constitutive model for metal deformation. Acta Metall. 28 (11), 1443–1465.
Govik, A., Rentmeester, R., Nilsson, L., 2014. A study of the unloading behaviour of dual phase steel. Mater. Sci. Eng. 602, 119–126.
Halilovič, M., Vrh, M., Štok, B., 2007. Impact of elastic modulus degradation on springback in sheet metal forming. AIP Conf. Proc. 908 (1), 925–930.
Halilovič, M., Vrh, M., Štok, B., 2008. Prediction of elastic strain recovery of a formed steel sheet considering stiffness degradation. Meccanica 44 (3), 321–338.
Hull, D., Bacon, D.J., 2011. Introduction to Dislocations, fifth ed. Elsevier, Oxford.
Kim, H., Kim, C., Barlat, F., Pavlina, E., Lee, M.G., 2013. Nonlinear elastic behaviors of low and high strength steels in unloading and reloading. Mater. Sci. Eng. 562, 161–171.
Lee, J., Lee, J.Y., Barlat, F., Wagoner, R.H., Chung, K., Lee, M.G., 2013. Extension of quasi-plasticelastic approach to incorporate complex plastic flow behavior application to springback of advanced high-strength steels. Int. J. Plast. 45, 140–159.
Lee, M.G., Kim, D., Kim, C., Wenner, M.L., Wagoner, R.H., Chung, K., 2007. A practical two-surface plasticity model and its application to spring-back prediction. Int. J. Plast. 23 (7), 1189–1212.
Li, K.P., Carden, W.P., Wagoner, R.H., 2002a. Simulation of springback. Int. J. Mech. Sci. 44 (1), 103–122.
Li, X., Yang, Y., Wang, Y., Bao, J., Li, S., 2002b. Effect of the material-hardening mode on the springback simulation accuracy of v-free bending. J. Mater. Process. Technol. 123 (2), 209–211.
Liu, Y.L., Zhu, Y.X., Dong, W.Q., Yang, H., 2013. Springback prediction model considering the variable young's modulus for the bending rectangular 3a21 tube. J. Mater. Eng. Perform. 22 (1), 9–16.
Mendiguren, J., Cortés, F., Galdos, L., Berveiller, S., 2013. Strain paths influence on the elastic behaviour of the TRIP 700 steel. Mater. Sci. Eng. 560, 433–438.
Mendiguren, J., Cortés, F., Gómez, X., Galdos, L., 2015. Elastic behaviour characterisation of TRIP 700 steel by means of loadingunloading tests. Mater. Sci. Eng. 634, 147–152.
Montgomery, D.C., Runger, G.C., Hubele, N.F., 2011. Engineering Statistics. Wiley.
Morestin, F., Boivin, M., 1996. On the necessity of taking into account the variation in the young modulus with plastic strain in elastic-plastic software. Nucl. Eng. Des. 162 (1), 107–116.
Mott, N.F., 1952. Cxvii. a theory of work-hardening of metal crystals. London Edinburgh Dublin Philosoph. Mag. J. Sci. 43 (346), 1151–1178.
Nguyen, N.T., Lee, M.G., Kim, J.H., Kim, H.Y., 2013. A practical constitutive model for AZ31b mg alloy sheets with unusual stressstrain response. Finite Elem. Anal. Des. 76, 39–49.
Pavlina, E.J., Lee, M.G., Barlat, F., 2015a. Observations on the nonlinear unloading behavior of advanced high strength steels. Metal. Mater. Trans. A 46 (1), 18–22.
Pavlina, E.J., Lin, C., Mendiguren, J., Rolfe, B.F., Weiss, M., 2015b. Effects of microstructure on the variation of the unloading behavior of DP780 steels. J. Mater. Eng. Perform. 24 (10), 3737–3745.
Pérez, R., Benito, J.A., Prado, J.M., 2005. Study of the inelastic response of TRIP steels after plastic deformation. ISIJ Int. 45 (12), 1925–1933.
Simo, J.C., Hughes, T.J.R., 2006. Computational Inelasticity, Vol. 7. Springer Science & Business Media.
Sun, L., Wagoner, R.H., 2011. Complex unloading behavior: nature of the deformation and its consistent constitutive representation. Int. J. Plast. 27 (7), 1126–1144.
Taylor, G.I., 1934. The mechanism of plastic deformation of crystals. part i. theoretical. Proc. R. Soc. London A 145 (855), 362–387.
Torkabadi, A., van Liempt, P., Meinders, V.T., van den Boogaard, A.H., 2015. Constitutive model for the anelastic behavior of advanced high strength steels. In: XIII International Conference on Computational Plasticity. CIMNE, pp. 378–385.
van Liempt, P., Sietsma, J., 2016. A physically based yield criterion i. determination of the yield stress based on analysis of pre-yield dislocation behaviour. Mater. Sci. Eng. 662, 80–87.
Viguier, B., 2003. Dislocation densities and strain hardening rate in some intermetallic compounds. Mater. Sci. Eng. 349 (12), 132–135.
Vrh, M., Halilovič, M., Mišič, M., Štok, B., 2008. Strain path dependent stiffness degradation of a loaded sheet. Int. J. Mater. Form. 1 (1), 297–300.
Vrh, M., Halilovič, M., Štok, B., 2011. The evolution of effective elastic properties of a cold formed stainless steel sheet. Exp. Mech. 51 (5), 677–695.
Wagoner, R.H., Lim, H., Lee, M.G., 2013. Advanced issues in springback. Int. J. Plast. 45, 3–20.
Wilkins, M.L., 1963. Calculation of elastic-plastic flow. In: Alder, B., Fernbach, S., Rotenberg, M. (Eds.), Methods in computational physics, Vol. 3. Academic Press New York.
Yang, M., Akiyama, Y., Sasaki, T., 2004. Evaluation of change in material properties due to plastic deformation. J. Mater. Process. Technol. 151 (13), 232–236.
Yeh, H.Y., Cheng, J.H., 2003. Nde of metal damage: ultrasonics with a damage mechanics model. Int. J. Solids Struct. 40 (26), 7285–7298.
Yoshida, F., Uemori, T., Fujiwara, K., 2002. Elastic-plastic behavior of steel sheets under in-plane cyclic tensioncompression at large strain. Int. J. Plast. 18 (56), 633–659.
Yu, H.Y., 2009. Variation of elastic modulus during plastic deformation and its influence on springback. Mater. Des. 30 (3), 846–850.
Zang, S.L., Liang, J., Guo, C., 2007. A constitutive model for spring-back prediction in which the change of young's modulus with plastic deformation is considered. Int. J. Mach. Tools Manuf 47 (11), 1791–1797.
Zener, C., 1948. Elasticity and Anelasticity of Metals. University of Chicago Press.